UNIABUJA Journal of Engineering and Technology

https://ujet.uniabuja.edu.ng/

ISSN: 2714-3236 (Online); 2714-3228 (Print)

Volume 3, Issue 2, 2026; 486-497

Physical, Mechanical, and Microstructural Characterization of Guinea Corn Husk Particleboards Bonded with Gum Arabic and Recycled PET

Victory KALU-MBA[1*], Emmanuel E. NDUBUBA[2], Olufunmilayo I. NDUBUBA[3]

[1*]*Risque et Environment, Ecole Centrale de Lyon, Lyon, France*
[2,3]*Department of Civil Engineering, University of Abuja, Abuja, Nigeria*

[1*]*victorykalumba14@gmail.com*, [2]*emmanuel.ndububa@uniabuja.edu.ng*, [3]*olufunmilayo.ndububa@uniabuja.edu.ng*

Abstract

Traditional wood-based particleboards (PBs) heavily rely on amino-formaldehyde synthetic resins, a paradigm that exacerbates global deforestation and presents severe carcinogenic health hazards via volatile emissions. To address these ecological and toxicological vulnerabilities, this study investigates a novel, eco-friendly composite architecture utilizing guinea corn husk (GCH) as a bio-based filler matrix, integrated with a hybrid binder system composed of polyethylene terephthalate (PET) and gum Arabic (GA). A systematic formulation strategy was deployed, maintaining a constant 70 wt.% GCH loading while systematically varying the PET-to-GA binder ratios across six discrete configurations: 0/30, 5/25, 10/20, 15/15, 20/10, and 25/5 wt.%. The resulting composites underwent comprehensive macro-characterization to quantify their physical and mechanical phenotypes, specifically analyzing bulk density, fluid transport kinetics (water absorption and thickness swelling), alongside quasi-static mechanical profiles (compressive strength, axial and split tensile strengths, flexural response, and modulus of elasticity). To elucidate the underlying structural mechanics, microstructural evolution and elemental distributions were mapped via scanning electron microscopy (SEM) and energy-dispersive X-ray spectroscopy (EDS). The hybrid panels demonstrated excellent hydro-resistance, restricting water absorption to 3.15–9.81% and thickness swelling to 3.58–9.02%. The empirical data reveals that escalating PET fractions dramatically optimize both the dimensional stability and the load-bearing capacity of the network through improved interfacial binding. Ultimately, these green composites successfully satisfy institutional threshold standards for non-load-bearing engineering applications, establishing a compelling, high-performance, and low-emission vanguard to displace legacy wood-formaldehyde panels.

Keywords: *Particle board, Guinea corn husk, Gum Arabic, Environmental sustainability, Waste polyethylene terephthalate bottles.*

1.0 Introduction

The global consumption of engineered lignocellulosic composites, particularly particleboards (PBs), continues to accelerate, propelled by accelerated urbanization and concurrent expansions within the infrastructural and cabinetry sectors. Historically, the architectural archetype of PBs relies on wood-derived particulate matrices consolidated via thermosetting synthetic resins, predominantly urea-formaldehyde (UF) and melamine-formaldehyde (MF) networks. While these synthetic matrices yield satisfactory mechanical profiles, their ubiquity across non-load-bearing applications including, interior architectural linings, modular partitions, cabinetry cores, and logistics packaging, exacerbates global deforestation and triggers profound toxicological anxieties. Chief among these is the chronic outgassing of volatile organic compounds (VOCs), specifically formaldehyde, an institutionalized human carcinogen. Consequently, engineering a transition toward circular, ecologically benign material alternatives has emerged as a critical imperative in sustainable materials design [1]. To mitigate these ecological liabilities, contemporary research has pivoted toward valorizing agricultural mass-residues and biopolymer binders to displace legacy timber and petrochemical resins. Lignocellulosic by-products such as rice husks, maize stalks, coir fibers, bagasse, and calcined marine shells have been extensively characterized as alternative filler phases due to their structural renewability, rich lignocellulosic architecture, and low cost. Integrating these agro-wastes into engineered panels simultaneously alleviates anthropomorphic pressure on forest ecosystems and curtails the environmental degradation associated with open-air incineration or landfilling of agricultural residues [2], [3], [4].

Within the domain of green adhesive engineering, Gum Arabic (GA) a complex, highly branched heteropolysaccharide exudate from *Acacia Senegal* has demonstrated significant efficacy as a binder owing to its inherent biodegradability, non-toxicity, and film-forming adhesive properties [5]. Nevertheless, the highly hydrophilic macromolecular structure of GA induces severe moisture sorption and subsequent hygrothermal swelling, compromising the long-term dimensional stability of the composite in humid environments. Prior investigations have sought to suppress this hydro-sensitivity by blending the biopolymer with hydrophobic

Received: 07-05-2026 / Accepted: 01-09-2026 / Published: 12-10-2026

https://doi.org/10.70118/ujet.2026.0302.39

agents, such as mineral waxes or recycled thermoplastic phases, to structurally shield the hydrophilic sites [5].

Concurrently, while binder modifications have advanced, guinea corn husk (GCH) a primary lignocellulosic residue derived from *Sorghum bicolor* processing remains heavily under-explored as a structural filler phase. In agrarian economies like Nigeria, GCH is generated in massive quantities, where it is routinely treated as a zero-value waste stream and subjected to open incineration. Given its robust cellulose and hemicellulose framework, GCH represents an ideal surrogate for timber particles; yet, its deployment within high-value material science frameworks remains scarce. Literature concerning the mechanical and microstructural synergy of GCH when coupled with non-toxic, waste-derived hybrid binder matrices is notably limited.

To bridge this literature gap, this study develops a novel, hybrid green composite utilizing a GCH filler matrix consolidated by a bi-phase binder system of Gum Arabic and recycled polyethylene terephthalate (PET), with the latter serving as a hydrophobic phase modifier. Operating at a fixed 70 wt.% GCH filler loading, we systematically manipulate the PET/GA mass fractions to establish their explicit influence on the resulting composite's mechanical, physical, and microstructural phenotypes. The scientific novelty of this intervention lies in the synergistic macromolecular interfacial binding achieved between GCH, GA, and PET. This approach simultaneously tackles agricultural waste management and plastic pollution, offering a high-performance, low-emission vanguard for non-structural engineering applications.

2.0 Materials and Methods

2.1 Material Preparation

The primary raw materials used in this study were guinea corn husk (GCH), waste polyethylene terephthalate (PET) bottles, Gum Arabic (GA), and water. The GCH was collected from a cattle feed market in Madalla, Niger State, Nigeria, where it is commonly sold as livestock fodder. Waste PET bottles were sourced from local plastic collectors operating within Abuja, Nigeria, ensuring the use of post-consumer plastic waste. Gum Arabic (GA) was procured from a local market in Suleja, Niger State, Nigeria, where it was sold in congealed ball-like forms typically ranging from 15 to 35 mm in diameter. The water used throughout the study was potable tap water.

To optimize interfacial bonding and ensure structural homogeneity within the composite matrix, the harvested raw materials were subjected to systematic size reduction and thermal pretreatment protocols. Both the guinea corn husk (GCH) filler and the recycled polyethylene terephthalate (PET) bottles underwent initial manual comminution, followed by mechanical milling. The resulting particulate matter was classified using a British Standard (BS) 2.0 mm mesh sieve to isolate a uniform particle size distribution optimal for consolidation (as illustrated in Figure 1 and Figure 2); the morphology of the crude Gum Arabic (GA) resin is depicted in Figure 3. This rigorous classification step was vital to eliminate packing density variations and ensure a contiguous, uniform phase distribution throughout the composite matrix [6] .

To mitigate the detrimental effects of volatile organic extractives, free sugars, and other chemical contaminants that typically inhibit polymer cross-linking, the sieved GCH and PET particles were subjected to a hydrothermal pretreatment. The particulate phases were immersed in a hot water bath maintained at 85°C for 60 minutes. Following this aqueous extraction process, the leachate was drained, and the materials were subjected to ambient air-drying for 72 hours until a stable, minimal moisture equilibrium was achieved.

This desiccation phase is fundamentally critical; excess residual moisture at the filler-binder interface induces steam pocket formation during hot pressing, which severely compromises subsequent adhesive wet-out and mechanical performance [6].

The crude, congealed nodules of Gum Arabic (GA) were initially subjected to manual comminution via mortar and pestle to yield a coarse powder. To control the particle size distribution and optimize the subsequent dissolution and blending kinetics, the pulverized GA was systematically classified using 150 µm and 75 µm British Standard (BS) sieves. The target fraction was strictly isolated by capturing the particles that permeated the 150 µm mesh but were retained on the 75 µm mesh (+75 µm / -150 µm). This specific geometric envelope was engineered to maximize the specific surface area of the biopolymer without inducing excessive agglomeration. Consequently, this precise particle size range facilitates a more homogenous distribution during dry blending, promoting optimal adhesive wet-out and bolstering the interfacial bonding mechanics within the heterogeneous GCH-PET composite matrix. Specific gravity tests were carried out on the GCH, PET and GA, respectively following ASTM D2395 [7]

Received: 07-05-2026 / Accepted: 01-09-2026 / Published: 12-10-2026

https://doi.org/10.70118/ujet.2026.0302.39

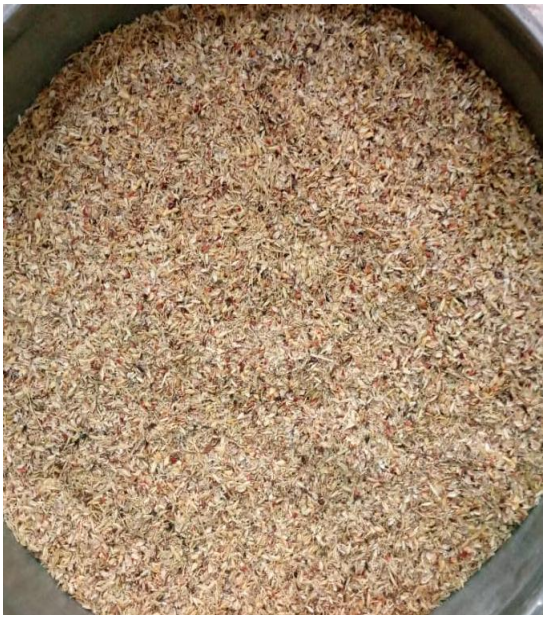


Figure 1. Prepared GCH



Figure 2. Prepared PET particles



Figure 3. GA resin binder

.

2.1.1 Mix Design and Particleboard Fabrication

To establish the experimental matrix, the guinea corn husk (GCH) was maintained at a constant 70% by weight in all mixes, while the proportions of Gum Arabic (GA) and polyethylene terephthalate (PET) were varied in the range of 0%, 5%, 10%, 15%, 20%, and 25%. These proportions were selected to assess the effect of binder variation on the performance of the particle board.

In developing this mix design, previous studies on GA-based particle boards (PBs) were consulted to identify performance benchmarks and contextualize the expected material behavior. Table 1 presents a summary of relevant results, including density, water absorption, and swelling in thickness, as reported in prior investigations involving GA and other biomass or plastic wastes [6], [8], [9], [10]. The sequence of preparation and experimental procedures followed in this study is summarized in the flowchart presented in Figure 4.

Received: 07-05-2026 / Accepted: 01-09-2026 / Published: 12-10-2026
https://doi.org/10.70118/ujet.2026.0302.39

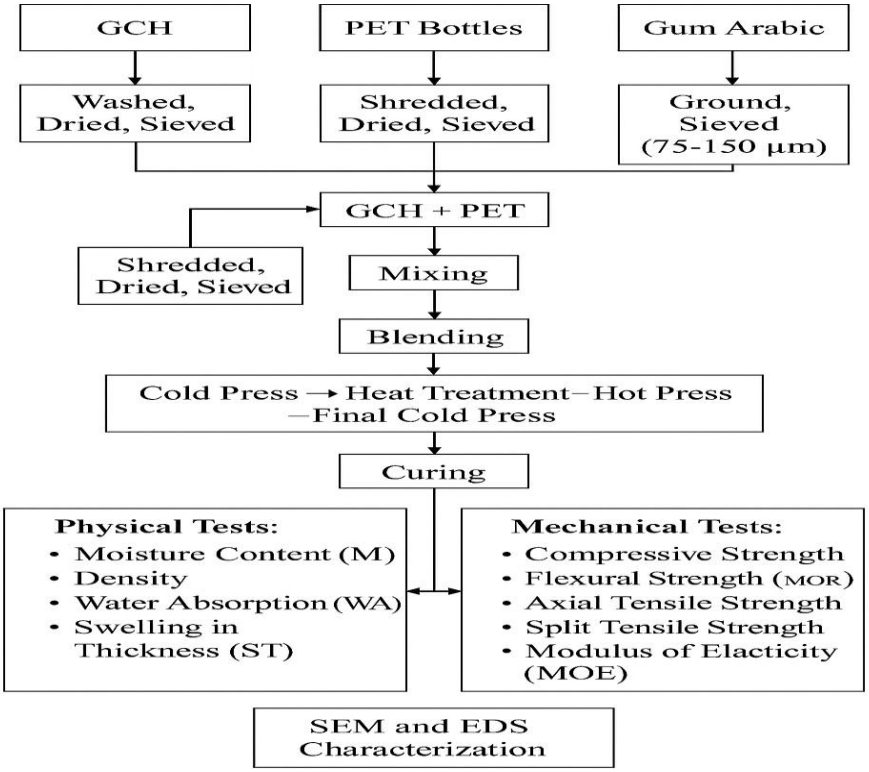


Figure 4. The sequence of preparation and experimental procedures followed

It is of interest to note that most PBs made from GA as binder fall within the high-density medium board (HDMB) classification, which ranges between 560–900 kg/m³ [11]. An outlier is the board using Ordinary Portland Cement (OPC) as the binder, which showed a significantly higher density (1281.1 - 1766 kg/m³) [8].

Table 1: Water Absorption and Swelling in Thickness from Previous Studies

PB Material	**Source**	**Density (Kg/m³)**	**Water Absorption (%) 2 min**	**Swelling in Thickness (%) 2 h**
OPC + SD + PSR	(Odeyemi et al., 2020)	1281.1- 1766	Minimum: 2.12	2.0 - 2.6
GA + RH + EPS	(Ndububa et al., 2023)	759.3 - 808.3	14.65 - 21.82	0.97 - 1.22
GA + RH + CW	(Raymond & Ndububa, 2023)	565.29 - 798.64	2.72 - 12.42	0.00 - 12.02
GA + CC	(Ndububa et al., 2006)	571.67- 816.67	-	-
GA + RH + SD	(Mas'ud & Ndububa, 2023)	447.71 - 698.84	7.62 - 12.67	7.60 - 12.33
GA + FH	(Ndububa et al., 2015)	213 – 580	-	-
GA + SD + WS	(Ndububa, 2013)	692 – 864	20.0 - 40.0	-
Standard Values	(BSI, 2003)	560 – 900	0.66 (BSI, 2003)	10 (24h) (BSI, 2003)

Note: RH - rice husk; SD - sawdust; EPS - expanded polystyrene; FH - fonio husk; WS - wood shavings; CW - candle wax; CC - corn cob; PSR - periwinkle shell residue.

The prepared components of the PB composites, GCH, GA and PET plastic were weighed and mixed in varying ratios. GCH constituted 70% while the remaining 30% was varied between PET and GA as shown in Table 2.

Table 2: Experimental design of particle boards

Sample PB	GCH (%)	PET (%)	GA (%)	Design ratio (GCH: PET: GAR)
PB1	70	0	30	1:0:0.43
PB2	70	5	25	1:0.07:0.36

Received: 07-05-2026 / Accepted: 01-09-2026 / Published: 12-10-2026

https://doi.org/10.70118/ujet.2026.0302.39

PB3	70	10	20	1:0.14:0.29
PB4	70	15	15	1:0.21:0.21
PB5	70	20	10	1:0.29:0.14
PB6	70	25	5	1:0.36:0.07

The materials were thoroughly mixed with the binder to ensure uniform distribution and consistency before being placed into 100 × 100 × 50 mm molds to form particle board mats. A custom four-stage pressing sequence was applied, developed through preliminary trials to suit the specific behavior of the GCH - GA - PET composite. The process began with cold pressing at 2.20 N/mm² to initiate densification and reduce mat thickness. This was followed by thermal treatment in an oven at 160°C for 2 hours, intended to evaporate residual moisture and soften the PET component, facilitating its bonding with the GCH matrix. A third phase of hot pressing at 2.20 N/mm² was then applied to further enhance interfacial bonding. Finally, a second cold pressing at 1.20 N/mm² was carried out to stabilize the board geometry during cooling and allow proper setting of the binder. While this sequence is not based on a formal standard, it was designed to optimize moisture removal, binder activation, and mechanical consolidation of the composite. The formed panels were conditioned at ambient temperature (25 ± 2°C) and relative humidity (26 ± 2%) prior to testing. Representative stages are shown in Figures 5 -7.



Figure 5. 100 x100 x 500 metal mould



Figure 6. Constituent materials ready for pressing



Figure 7. Samples of PB

2.2 Physical and Durability Tests

Physical and durability tests conducted on the particle boards included moisture content, density, water absorption, and swelling in thickness. Moisture content was determined following [12], [13] by oven-drying the samples at 105°C for 24 hours and calculating the percentage weight difference. Density was calculated from the measured mass and volume of the samples. Water absorption and swelling in thickness were evaluated in accordance with [14], [15], respectively, by immersing test specimens in water and measuring the increase in mass and thickness after specified time intervals.

Received: 07-05-2026 / Accepted: 01-09-2026 / Published: 12-10-2026
https://doi.org/10.70118/ujet.2026.0302.39

2.3 Mechanical Tests

Mechanical tests carried out on the particle boards included compressive strength, flexural strength, axial tensile strength, splitting tensile strength, and modulus of elasticity. Compressive strength was evaluated using cube samples under uniaxial loading in accordance with [16], [17]. Flexural strength (modulus of rupture) was measured using center-point loading according to [18]. Axial tensile strength was determined based on [11], [19], while splitting tensile strength followed [16]. The modulus of elasticity was derived from the linear portion of the flexural stress-strain curve as in [12], [20].

2.4 Microstructural analysis and elemental composition determination

Microstructural characterization of the particle boards was carried out using Scanning Electron Microscopy (SEM), while elemental composition was determined using Energy Dispersive X-ray Spectroscopy (EDS). SEM analysis was performed at the Electron Microscopy Laboratory, NSRMEA Kaduna, Nigeria, to observe the internal morphology, surface texture, and distribution of components within the composite matrix. Samples approximately 2-5 mm in size were mounted on aluminum stubs using carbon adhesive and examined under varying magnifications. EDS analysis was conducted on the same samples using a system operated at an accelerating voltage of 15 kV to identify and quantify the elemental composition[10], [17] .

3.0 Results and Discussion

3.1 Physical Properties and Water Absorption Behaviour

The specific gravities of GCH, PET, and GA were 0.67, 1.05, and 1.34, respectively. Particle size analysis showed that GCH ranged from 0.075-2.36 mm, PET from 0.15 - 1.18 mm, and GA crystals from 4.75-28 mm, although GA was transformed into resin prior to use. The relatively high specific gravity of GA indicated its potential to increase the overall density of the particle boards.

Table 3 presents the moisture content, density, water absorption (WA), and swelling in thickness (ST) values for each sample. Moisture content decreased with increasing PET content, ranging from 12.1% (PB1) to 7.6% (PB6). This trend is consistent with the hydrophobic nature of PET and the hydrophilic nature of GA, confirming PET's role in moisture resistance *[21], [22], [23]*. All samples met the permissible moisture range defined by [24], [25], though only PB6 complied with the stricter limit of 10% [15].

Density values ranged from 930.5 kg/m³ (PB1) to 737.5 kg/m³ (PB6), decreasing with higher PET content. This is attributed to the lower specific gravity of PET compared to GA. Samples PB3 to PB6 met the density ranges set by IS 3087 (500 - 900 kg/m³) and BS EN 316 (≥560 kg/m³), while PB1 to PB4 also exceeded the ANSI threshold (≥800 kg/m³) for high-density boards. Comparisons with similar studies involving GA and agro-waste fillers *[3], [6], [9], [10]* confirm that the GCH-based boards achieved competitive density profiles.

Water absorption results showed a decreasing trend with increasing PET content. The lowest WA (3.15%) was recorded for PB5, while PB1 absorbed 9.81% water within 2 minutes. The WA behaviour is attributed to PET's hydrophobicity, which limits moisture ingress, whereas GA promotes water uptake due to its polysaccharide nature. These findings align with previous works where hydrophobic additives such as candle wax or PET improved water resistance in GA-based composites *[18], [26]*.

Swelling in thickness followed a similar trend. PB3, PB4, and PB5 recorded ST values of 9.02%, 4.52%, and 3.58%, respectively, while PB1, PB2, and PB6 disintegrated during the test. Though ANSI A208.1 sets a 24-hour swelling limit of 8%, the 2-hour test duration in this study was chosen to avoid further disintegration. The optimal performance of PB5 suggests a favourable PET-to-GA balance. Supporting literature *[27], [28], [29]* shows that stabilizing GA with hydrophobic materials significantly improves dimensional stability. Therefore, combining PET with additional hydrophobic agents like candle wax may yield even better performance.

Table 3*:* Physical and durability test results of PB samples

Sample PB	Moisture content (%)	Density (Kg/m³)	2 mins Water Absorption (%)	2 hrs. Swelling in thickness (%)
PB1	12.1	930.5	9.81	Disintegrated
PB2	11.9	906.3	5.11	Disintegrated
PB3	11.4	883.9	5.43	9.02
PB4	10.9	813.4	4.49	4.52
PB5	10.6	790.2	3.15	3.58
PB6	7.6	737.5	3.66	Disintegrated

Received: 07-05-2026 / Accepted: 01-09-2026 / Published: 12-10-2026

https://doi.org/10.70118/ujet.2026.0302.39

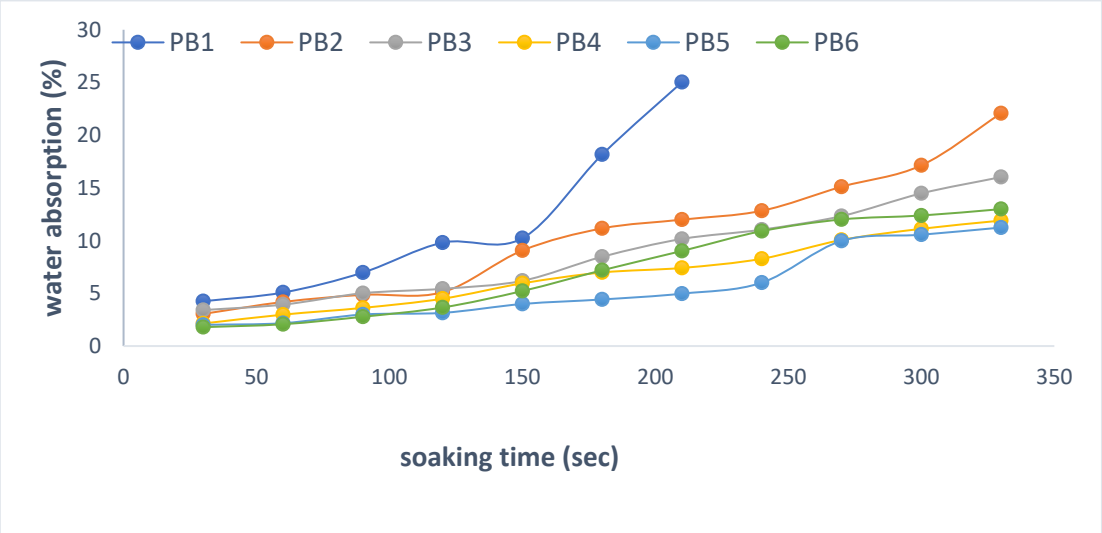


Figure 8. Water absorption trend of samples

Figures 8 illustrates water absorption behaviour over time. The trend indicates increased water uptake with time and decreasing PET content. Samples PB4 to PB6 showed early plateauing after 300 seconds, suggesting saturation.

3.3 Mechanical Properties of the Produced Particle

Table 4 presents the average values of compressive strength, modulus of rupture, axial tensile strength, split tensile strength, and modulus of elasticity for the various particle board (PB) formulations. These results reveal key performance trends linked to the mix proportions of PET and GA in the matrix.

Compressive strength values ranged from 4.01 N/mm² for PB1 to 7.16 N/mm² for PB4 shown in Figure 9. A parabolic trend was observed, with strength increasing with PET content up to a certain point (PB4), beyond which further addition of PET led to a decline. This aligns with the optimal binder-to-filler ratio principle, where excess PET may hinder uniform bonding due to poor dispersion. Compared to previous studies on fonio husk/GA and rice husk/GA-wax composites, which reported compressive strengths below 4.0 N/mm², the current values reflect the enhanced bonding contribution of PET, particularly at balanced ratios with GA.

Modulus of rupture (MOR), a measure of flexural strength, followed a similar pattern, peaking at 12.1 N/mm² in PB5. This value exceeded the BS EN 622-5 minimum requirement of 6 N/mm² for UL1-type MDF boards and surpassed those recorded in comparable agro-waste particleboard studies[13]. However, while PB5 exhibited the highest MOR, its modulus of elasticity (MOE) was lower than that of PB4 (376.69 N/mm² vs. 575.76 N/mm²). This suggests a more brittle fracture behavior for PB5, likely due to rapid crack propagation through a stiffer matrix lacking sufficient energy absorption. The higher MOE of PB4 indicates a more ductile matrix response with greater ability to withstand deformation before failure, consistent with its balanced PET-GA composition and SEM-observed compact microstructure.

Axial tensile strength increased from 1.22 N/mm² in PB1 to 3.34 N/mm² in PB5, again showing PET's positive contribution to tensile performance. The values across all samples were significantly higher than those reported for rice husk or fonio husk GA-based boards, demonstrating the effectiveness of PET as a reinforcing stabilizer. An unexpected result was observed in PB1, which, despite having the lowest compressive strength and disintegrating in water, recorded a relatively high split tensile strength of 8.20 N/mm². This discrepancy may be attributed to localized surface densification and binder concentration during pressing, allowing the board to resist diagonal tension under dry testing conditions. The disintegration of PB1 in water is likely linked to internal cohesion loss, which did not affect its short-term dry mechanical response. This observation emphasizes that moisture durability and mechanical strength, especially split tensile resistance, do not always correlate directly in moisture-sensitive composites.

MOE results generally followed the trend of MOR and compressive strength, peaking at PB4 (575.76 N/mm²) and decreasing thereafter. While MOE values are often used to infer stiffness, the deviation in PB5 can be attributed to microstructural variations and possible brittle failure, as observed in SEM analysis and inferred from the steep flexural load-deflection profile. These results still met the British standard threshold (≥510 N/mm² for 19 - 30 mm thick dry-use MDF), confirming suitability for non-load bearing applications like partitioning and interior finishes.

Received: 07-05-2026 / Accepted: 01-09-2026 / Published: 12-10-2026
https://doi.org/10.70118/ujet.2026.0302.39

Table 4: Mechanical properties test results of samples

Sample PB	Compressive strength (N/mm²)	Modulus of rupture (N/mm²)	Axial tensile strength (N/mm²)	Split tensile strength (N/mm²)	Modulus of Elasticity (N/mm²)
PB1	4.01	5.5	1.22	8.20	499.00
PB2	5.32	7.7	2.89	9.28	428.79
PB3	5.97	9.6	2.01	9.87	547.27
PB4	7.16	11.3	3.12	10.75	575.76
PB5	6.05	12.1	3.34	9.48	376.69
PB6	4.42	6.8	2.92	7.64	334.51

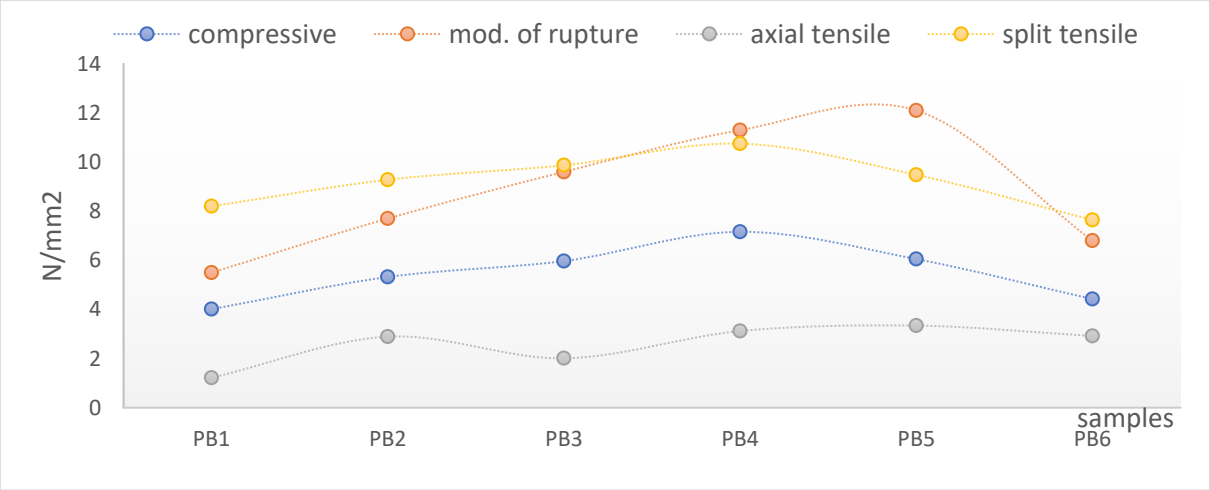


Figure 9. Trends in mechanical properties

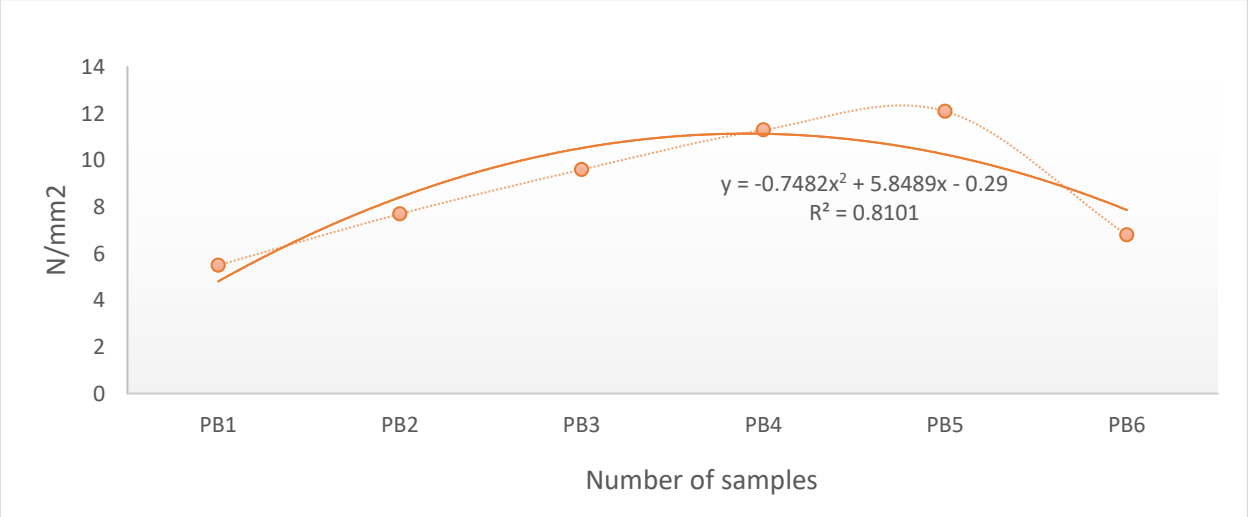


Figure 10. Trend in flexural strength property

Overall, mechanical performance was optimized in PB4 and PB5, where PET and GA contents were nearly equal. The SEM micrographs support these findings, showing reduced voids and better particle-matrix integration in these samples. The trendline modeling showed quadratic relationships for most mechanical parameters in Figure 10, although the R^2 value of 0.81 for MOE prediction indicates moderate reliability.

3.4 Micro-Structural and Chemical Characterization of the Particle Board Samples

3.4.1 Micro-structural characterization:

The SEM analysis revealed notable variations in microstructural integrity across the particle board samples. Quantitative image assessment was conducted to evaluate porosity levels, crack morphology, and interfacial bonding within the composite matrix. Key parameters measured include average porosity percentage, minimum - maximum crack width, and observable matrix - fiber interactions.

Received: 07-05-2026 / Accepted: 01-09-2026 / Published: 12-10-2026
https://doi.org/10.70118/ujet.2026.0302.39

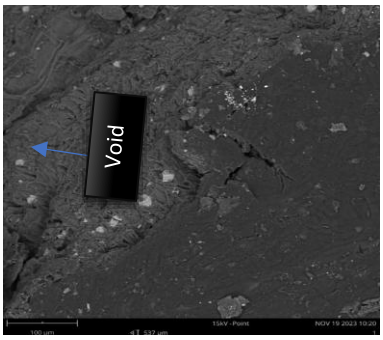


Figure 11. SEM Mirograph of PB1

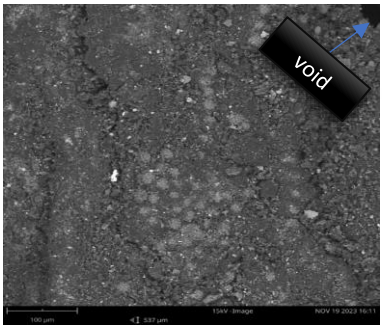


Figure 12. SEM micrograph of PB2



Figure 13. SEM micrograph of PB3

PB1 (Figure 11), PB2 (Figure 12), and PB6 (Figure 16) exhibited high porosity with widespread surface cracks, with average pore areas exceeding 12% of the scanned field. Crack widths in these samples ranged from approximately 40 µm to 140 µm, contributing to the observed poor mechanical performance and moisture resistance. In particular, PB1 showed loose bonding regions and weak interfacial adhesion between PET particles and the GCH matrix, as evidenced by fragmented boundaries and unfilled voids. This helps explain its disintegration in water despite its unexpectedly high split tensile strength, which may have been supported by surface densification alone.

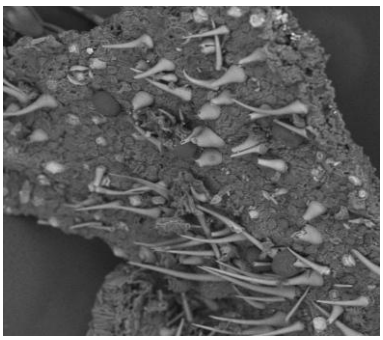


Figure 14. SEM micrographs of PB4

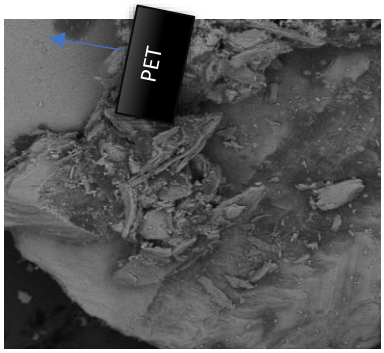


Figure 15. SEM micrograph of PB5

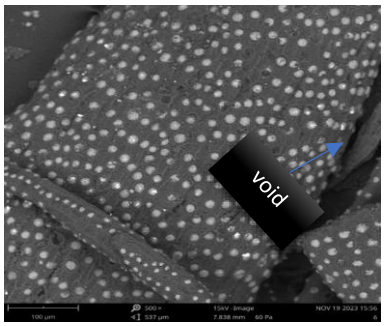


Figure 16. SEM micrograph of PB6

In contrast, PB3 (Figure 13), PB4 (Figure 14), and PB5 (Figure 15) exhibited denser microstructures with fewer and narrower cracks, typically within 10 - 35 µm range. The matrix in these samples showed well-distributed PET and GA content with smoother transitions at the fibre binder interface, indicating effective bonding. PB4 presented the most compact structure with the lowest observed porosity (less than 5%) and minimal void interconnectivity. The improved load transfer efficiency and interfacial integrity in PB4 likely contributed to its superior modulus of elasticity and overall mechanical performance.

These observations confirm that porosity and crack geometry are critical indicators of board integrity and that optimized PET/GA ratios reduce internal defects and enhance structural bonding. The SEM-based microstructural trends closely align with the mechanical and physical test results, reinforcing the importance of matrix homogeneity and binder distribution in agro-waste-based particleboard systems.

These findings are consistent with [29], who reported that compact microstructures with reduced void content in macadamia nutshell/GA boards corresponded directly to superior flexural and compressive performance. Similarly, Raymond and Ndububa [9] observed that improved binder distribution in rice husk/GA/candle wax boards produced denser matrices with fewer cracks, which translated to better dimensional stability a pattern mirrored in the present study's PB4 and PB5 formulations. The crack widths observed in the poorly performing samples (40 -140 µm in PB1, PB2, and PB6) are notably wider than those reported by Ndububa et al. for GA/rice husk/EPS boards, suggesting that the absence of a balanced PET- GA ratio in those extremes creates interfacial weakness not compensated by individual constituent properties alone.

Received: 07-05-2026 / Accepted: 01-09-2026 / Published: 12-10-2026
https://doi.org/10.70118/ujet.2026.0302.39

3.4.2. Chemical composition characterization:

The elemental composition of the particle board samples, determined by Energy-Dispersive X-ray Spectroscopy (EDS), is presented in Table 5. Carbon was the predominant element across all samples, with its concentration increasing from 52.54% in PB1 to a peak of 76.77% in PB4 before declining to 61.84% in PB6. This distribution aligns partially with the mechanical performance trends, particularly in PB4, which exhibited a balanced PET- GA mix and the highest modulus of elasticity (MOE).

The elevated carbon levels are likely attributable to the high organic content of both PET and GCH, particularly following thermal processing. However, while a general association exists between carbon-rich matrices and improved mechanical behavior in polymer composites [30], elemental carbon percentage alone does not directly confirm bonding quality or mechanical strength. The presence of silicon was most notable in PB1 (27.33%), potentially due to inherent silica content in GCH. While silicon-bearing compounds can contribute to pozzolanic reactions in cementitious systems, the absence of confirmatory phase analysis limits any conclusive interpretation of pozzolanic behavior in this context.

The detected nitrogen mass fractions, which spanned a range of 14.50 wt.% to 22.11 wt.%, are hypothesized to originate from the thermal degradation and evolution of organic constituents during heat treatment, alongside potential trace nitrogenous species within the recycled polymer and biopolymer phases. Other detected elements, including aluminum, iron, magnesium, and phosphorus, were recorded in trace concentrations. These minor elemental signatures likely reflect endogenous mineral residuals inherent to the lignocellulosic biomass matrix or negligible contaminants introduced during mechanical processing. The structural dominance of elemental carbon across all composite formulations is highly consistent with the empirical trends reported by [17] for Gum Arabic/rice husk/sawdust panels. In both cases, the carbon profile fundamentally mirrors the intrinsically organic architecture of the agricultural filler and the polysaccharide-based natural binder network.

Crucially, the pronounced silicon concentration identified in formulation PB1 (27.33 wt.%) corroborates established literature on guinea corn husk (GCH) and related *Sorghum*-derived biomass, which natively sequester significant biogenic silica (SiO_2) within their cellular frameworks. However, in contrast to inorganic or cementitious systems where amorphous silica drives mechanical optimization via pozzolanic reactions, a parallel reinforcing mechanism cannot be definitively validated within this hybrid polymeric matrix [3], [9], [18].

The behavior of high-performance polymer-matrix composites, where elemental carbon abundance directly indexes the density of the interfacial organic networks. In formulation PB4, this elevated carbon mass fraction primarily denotes a higher volume fraction of recycled PET, which provides a continuous, hydrophobic phase that encapsulates the lignocellulosic GCH particles. This optimal distribution enhances interfacial stress transfer across the filler-matrix boundary and minimizes microstructural voids. Similar structural trends have been reported in related agro-waste composite literature, where maximizing the synthetic or natural polymer fraction within its optimal threshold yields a more cohesive, load-bearing matrix capable of efficiently mitigating crack propagation under tensile and flexural loads [30] .

Table 5: Elemental composition of the board samples

Element name	Weight concentration (%)					
	Sample ID					
	PB1	PB2	PB3	PB4	PB5	PB6
Carbon	52.54	64.00	64.44	76.77	66.66	61.84
Silicon	27.33	3.61	5.98	6.49	10.44	13.77
Nitrogen	14.50	18.44	22.11	12.35	17.07	15.83
Aluminum	0.96	1.18	1.46	1.45	0.75	0.72
Potassium	0.86	2.43	1.28	0.61	0.92	1.89
Iron	0.78	4.05	1.97	0.32	1.24	0.90
Sodium	0.70	0.41	0.36	0.29	0.45	0.74
Chlorine	0.59	0.76	0.61	0.25	0.45	0.61
Magnesium	0.52	0.95	0.47	0.41	0.58	1.38
Phosphorus	0.50	0.75	0.52	0.35	0.49	1.04
Sulfur	0.40	0.32	0.42	0.16	0.59	0.36
Calcium	0.31	1.91	0.38	0.00	0.28	0.92
Titanium	0.00	1.19	0.00	0.55	0.00	0.00

4.0 Conclusion

This research successfully demonstrates the viability of engineering value-added, green particleboards by utilizing guinea corn husk (GCH) as a bio-derived filler phase, consolidated via an innovative hybrid binder matrix of Gum Arabic (GA) and recycled polyethylene terephthalate (PET). The

Received: 07-05-2026 / Accepted: 01-09-2026 / Published: 12-10-2026

https://doi.org/10.70118/ujet.2026.0302.39

developed panels exhibit critical physical and mechanical profiles that successfully align with institutional threshold benchmarks, satisfying major British/European (EN) and American (ANSI) standardized classifications. Crucially, by manipulating the filler-to-binder mass fractions, the resulting composites can be tailored across low-, medium-, and high-density classifications, offering tunable structural configurations for diverse engineering requirements.

A pivotal finding of this investigation lies in the synergistic integration of recycled PET within the biopolymeric GA matrix. At near-equal polymeric proportions, the hydrophobic thermoplastic phase effectively shields the hydrophilic biopolymer sites, significantly suppressing moisture transport kinetics and upgrading the quasi-static mechanical capacity of the network. This macro-performance enhancement is directly validated by microstructural morphology, where optimal formulations reveal a highly cohesive microstructure characterized by minimized void volume fractions, narrowed micro-crack propagation widths, and superior interfacial filler-matrix encapsulation.

However, despite these promising mechanical phenotypes, applications in high-humidity or structural load-bearing zones demand strict caution, as lower PET concentrations leave the hydrophilic GA binder susceptible to moisture-induced degradation. Furthermore, while elemental mapping confirmed substantial carbon and biogenic silicon mass fractions, a precise chemical cross-linking or pozzolanic reaction mechanism cannot be definitively stated based on this data alone.

To fully resolve these interfacial bonding mechanics, secondary phase-compositional characterizations, specifically X-ray diffraction (XRD), Fourier-transform infrared spectroscopy (FTIR), and thermogravimetric analysis (TGA) are strongly recommended for subsequent iterations of this research. Future investigations should employ advanced mathematical tools—such as Response Surface Methodology (RSM), Taguchi robust design, or machine learning-driven numerical optimization algorithms—to map the multi-variable design space. This will systematically isolate the precise binder-to-filler stoichiometry required to achieve a Pareto-optimal balance between mechanical load-bearing capacity, dimensional stability, and hydro-resistance.

In summary, the GCH/GA-PET hybrid architecture introduces a compelling, eco-benign, and low-cost vanguard to displace conventional wood-formaldehyde panels. By intercepting both agricultural mass-waste and post-consumer plastic waste streams, this material offers a circular economy paradigm shift for non-structural and interior architectural applications.

References

[1] Sivadas, D. (2022). Pathways for sustainable economic benefits and green economies in light of the state of world forests 2022.

[2] Singh, M., Shahina, N. N., Das, S., Arshad, A., Siril, S., Barman, D., ... & Chakravarty, S. (2022). Forest resources of the world: present status and future prospects. *Land Degradation Neutrality: Achieving SDG 15 by Forest Management*, 1-23.

[3] Ndububa, E. E., & Oke, C. (2006). O and Ndububa OI "Mechanical Properties of Particleboards Produced from Maize Cobs with Gum Arabic as Resin Adhesive Binder". In *Proceedings of the 7th International Conference of the Nigerian Institution of Agricultural Engineers, Zaria, Nigeria* (Vol. 28, pp. 399-403).

[4] Odeyemi, S. O., Abdulwahab, R., Adeniyi, A. G., & Atoyebi, O. D. (2020). Physical and mechanical properties of cement-bonded particle board produced from African balsam tree (Populous Balsamifera) and periwinkle shell residues. *Results in Engineering*, *6*, 100126.

[5] Chaiklieng, S., Tongsantia, U., & Autrup, H. N. (2021). Risk assessment of inhalation exposure to formaldehyde among workers in medical laboratories. *Asia-Pacific Journal of Science and Technology*, *26*(4), 4-26.

[6] Ndububa, E., Muhammad, I., Sanusi, A., & Adeleke, W. (2023). The impact of expanded polystyrene on the performance characteristics of rice husk particleboard using gum arabic as adhesive binder. *Nile J Eng Appl Sci*, (1).

[7] ASTM, D. (2017). 2395-93. Standard test methods for specific gravity of wood and wood—based materials. *ASTM International: West Conshohocken, PA, USA*.

[8] Odeyemi, S. O., Abdulwahab, R., Adeniyi, A. G., & Atoyebi, O. D. (2020). Physical and mechanical properties of cement-bonded particle board produced from African balsam tree (Populous Balsamifera) and periwinkle shell residues. *Results in Engineering*, *6*, 100126.

[9] Raymond, S. P., & Ndububa, E. E. (2023). Performance Characterisation of Gum Arabic Bonded Particle Board Made from Rice Husk and Candle Wax. *Open Journal of Engineering Science (ISSN: 2734-2115)*, *4*(2), 50-73.

Received: 07-05-2026 / Accepted: 01-09-2026 / Published: 12-10-2026

https://doi.org/10.70118/ujet.2026.0302.39

[10] Ndububa, E., Muhammad, I., Sanusi, A., & Adeleke, W. (2023). The impact of expanded polystyrene on the performance characteristics of rice husk particleboard using gum arabic as adhesive binder. *Nile J Eng Appl Sci*, (1).
[11] EN, S. (2009). 622-5: 2009; Fibreboards—Specifications—Part 5: Requirements for Dry Process Boards (MDF). *Schweizerischer Ingenieurund Architekten-Verein SIA: Zürich, Switzerland*.
[12] Bhaduri, S. K., & Mojumder, P. (2008). Medium density particle board from Khimp plant. *Nat. Prod. Radiance*, *7*(2), 106-110.
[13] EN, B. (2009). 622-5. *Fibreboards, specifications. requirements for dry process boards (MDF)*.
[14] British Standards Institution. (1993). *Particleboards and fibreboards. Determination of swelling in thickness after immersion in water*. British Standards Institution.
[15] Bennett, J., Butler, J., Jones, B., & Sutherland, E. (2022). Straw Construction in the UK. *Technical Guide*.
[16] Iso, E. N. (2012). 527-2; Plastics—Determination of Tensile Properties—Part 2: Test Conditions for Moulding and Extrusion Plastics. *Organization of Standardization: Geneva, Switzerland*.
[17] Mas' Ud, A., & Ndububa, E. E. (2023). Engineering Characterization of Gum Arabic Bonded Particle Board Made from Rice Husk and Sawdust. *Open Journal of Engineering Science (ISSN: 2734-2115)*, *4*(1), 19-35.
[18] Ndububa, E. E. (2013). Performance characteristics of gum arabic bonded particleboard made from sawdust and wood shavings. *Ife Journal of Technology*, *22*(1), 5-8.
[19] Iso, E. (2012). 527-1; Plastics—Determination of Tensile Properties—Part 1: General Principles. *International Organization of Standardization: Geneva, Switzerland*.
[20] Suffian, M., Ormondroyd, G. A., & Hale, M. D. (2010). Comparisons of particleboard produced from Acacia hybrid and a UK commercial particleboard furnish from recycled wood. *Journal of Tropical Forest Science*, 227-236.
[21] Phillips, G. O., & Williams, P. A. (Eds.). (2009). *Handbook of hydrocolloids*. Elsevier.
[22] Wiles, D. M., & Scott, G. (2006). Polyolefins with controlled environmental degradability. *Polymer degradation and stability*, *91*(7), 1581-1592.
[23] Faruk, O., Bledzki, A. K., Fink, H. P., & Sain, M. (2012). Biocomposites reinforced with natural fibers: 2000–2010. *Progress in polymer science*, *37*(11), 1552-1596.
[24] Latifi, M. (Ed.). (2021). *Engineered polymeric fibrous materials*. Woodhead Publishing.
[25] British Standards Institution. (1993). *Particleboards and fibreboards. Determination of swelling in thickness after immersion in water*. British Standards Institution.
[26] Halvarsson, S., Edlund, H., & Norgren, M. (2009). Manufacture of non-resin wheat straw fibreboards. *Industrial crops and products*, *29*(2-3), 437-445.
[27] Móczó, J., & Pukánszky, B. (2019). Particulate filled polypropylene: structure and properties. In *Polypropylene handbook: morphology, blends and composites* (pp. 357-417). Cham: Springer International Publishing.
[28] Surdi, P. G., Bortoletto, G., Castro, V. R. D., Brito, F. M. S., Berger, M. D. S., & Zanuncio, J. C. (2019). Particleboard production with residues from mechanical processing of Amazonian woods. *Revista Árvore*, *43*(1), e430102.
[29] Mirindi, D., Onchiri, R. O., & Thuo, J. (2021). Physico-mechanical properties of particleboards produced from macadamia nutshell and gum arabic. *Applied sciences*, *11*(23), 11138.
[30] Mirdehghan, S. A. (2021). Fibrous polymeric composites. In *Engineered polymeric fibrous materials* (pp. 1-58). Woodhead Publishing.

Received: 07-05-2026 / Accepted: 01-09-2026 / Published: 12-10-2026

https://doi.org/10.70118/ujet.2026.0302.39